Molecular Therapy
Original Article

A replicating LCMV-based vaccine for the treatment of solid tumors

Mette-Triin Purde,[1] Jovana Cupovic,[1,12] Yannick A. Palmowski,[2] Ahmad Makky,[2] Sarah Schmidt,[3] Alexander Rochwarger,[2] Fabienne Hartmann,[1] Felix Stemeseder,[3] Alexander Lercher,[4] Marie-Therese Abdou,[1] David Bomze,[1] Lenka Besse,[5,13] Fiamma Berner,[1] Thomas Tüting,[6] Michael Hölzel,[7] Andreas Bergthaler,[4] Stefan Kochanek,[8] Burkhard Ludewig,[1] Henning Lauterbach,[3] Klaus K. Orlinger,[3] Tobias Bald,[9,14] Andrea Schietinger,[10] Christian Schürch,[2] Sandra S. Ring,[1,15,17] and Lukas Flatz[1,11,16,17]

[1]Institute of Immunobiology, Kantonsspital St. Gallen, 9007 St. Gallen, Switzerland; [2]Department of Pathology and Neuropathology, University Hospital and Comprehensive Cancer Center Tübingen, 72076 Tübingen, Germany; [3]Hookipa Pharma Inc., New York, NY 10118, USA; [4]Research Center for Molecular Medicine (CeMM) of the Austrian Academy of Sciences, 1090 Vienna, Austria; [5]Laboratory of Experimental Oncology, Department of Oncology and Hematology, Kantonsspital St. Gallen, 9007 St. Gallen, Switzerland; [6]Laboratory of Experimental Dermatology, Department of Dermatology, University Hospital Magdeburg, 39120 Magdeburg, Germany; [7]Institute of Experimental Oncology, University Hospital Bonn, 53127 Bonn, Germany; [8]Department of Gene Therapy, Ulm University, 89081 Ulm, Germany; [9]QIMR Medical Research Institute, Herston, QLD 4006, Australia; [10]Memorial Sloan Kettering Cancer Center, New York, NY 10065, USA; [11]Department of Dermatology, Kantonsspital St. Gallen, 9007 St. Gallen, Switzerland

Harnessing the immune system to eradicate tumors requires identification and targeting of tumor antigens, including tumor-specific neoantigens and tumor-associated self-antigens. Tumor-associated antigens are subject to existing immune tolerance, which must be overcome by immunotherapies. Despite many novel immunotherapies reaching clinical trials, inducing self-antigen-specific immune responses remains challenging. Here, we systematically investigate viral-vector-based cancer vaccines encoding a tumor-associated self-antigen (TRP2) for the treatment of established melanomas in preclinical mouse models, alone or in combination with adoptive T cell therapy. We reveal that, unlike foreign antigens, tumor-associated antigens require replication of lymphocytic choriomeningitis virus (LCMV)-based vectors to break tolerance and induce effective antigen-specific $CD8^+$ T cell responses. Immunization with a replicating LCMV vector leads to complete tumor rejection when combined with adoptive TRP2-specific T cell transfer. Importantly, immunization with replicating vectors leads to extended antigen persistence in secondary lymphoid organs, resulting in efficient T cell priming, which renders previously "cold" tumors open to immune infiltration and reprograms the tumor microenvironment to "hot." Our findings have important implications for the design of next-generation immunotherapies targeting solid cancers utilizing viral vectors and adoptive cell transfer.

INTRODUCTION

The emergence, growth, spread, and destruction of tumors represents the outcome of a complex and ongoing interaction between malignant cell masses and the host immune system. Describing the steps required for a successful antitumor immune response, the cancer-immunity cycle was proposed in 2013:[1] first, the release of tumor antigens from dying tumor cells leads to their uptake by antigen-presenting cells (APCs) and presentation to T cells, activating the latter; then, the activated tumor-antigen-specific T cells traffic to the tumor, infiltrate it, and kill further tumor cells, thereby releasing more tumor antigen and repeating the cycle. Early attempts to stimulate this cycle using immunotherapies revealed multiple challenges and led to the identification of significant obstacles to success, including the dominant role of tumor-induced immunosuppression, existing tolerance to tumor-associated antigens, and exclusion of T cells from established tumors.[2] Still, despite a further decade of research, the "recipe" for a successful immunotherapy able to help a broad population of patients, regardless of tumor or human leukocyte antigen (HLA) type, has yet to be defined.

The majority of cancer immunotherapies aim to prompt the host immune system to kill tumor cells by targeting either tumor-specific antigens, which are novel within the body, or tumor-associated antigens, which are also expressed in healthy tissues. In the latter case, there are

Received 17 April 2023; accepted 30 November 2023;
https://doi.org/10.1016/j.ymthe.2023.11.026.

[12]Present address: Max Planck Institute of Immunology and Epigenetics, 79108 Freiburg, Germany

[13]Present address: Department of Biology, Faculty of Medicine, Masaryk University, 625 00 Brno, Czechia

[14]Present address: Institute of Experimental Oncology, University Hospital Bonn, 53127 Bonn, Germany

[15]Present address: TranslaTUM, TU München, 81675 Munich, Germany

[16]Present address: Department of Dermatology, University Hospital Tübingen, 72016 Tübingen, Germany

[17]These authors contributed equally

Correspondence: Lukas Flatz, MD, University Hospital Tübingen, Department of Dermatology, 72016 Tübingen, Germany.
E-mail: lukas.flatz@med.uni-tuebingen.de

Please cite this article in press as: Purde et al., A replicating LCMV-based vaccine for the treatment of solid tumors, Molecular Therapy (2023), https://doi.org/10.1016/j.ymthe.2023.11.026

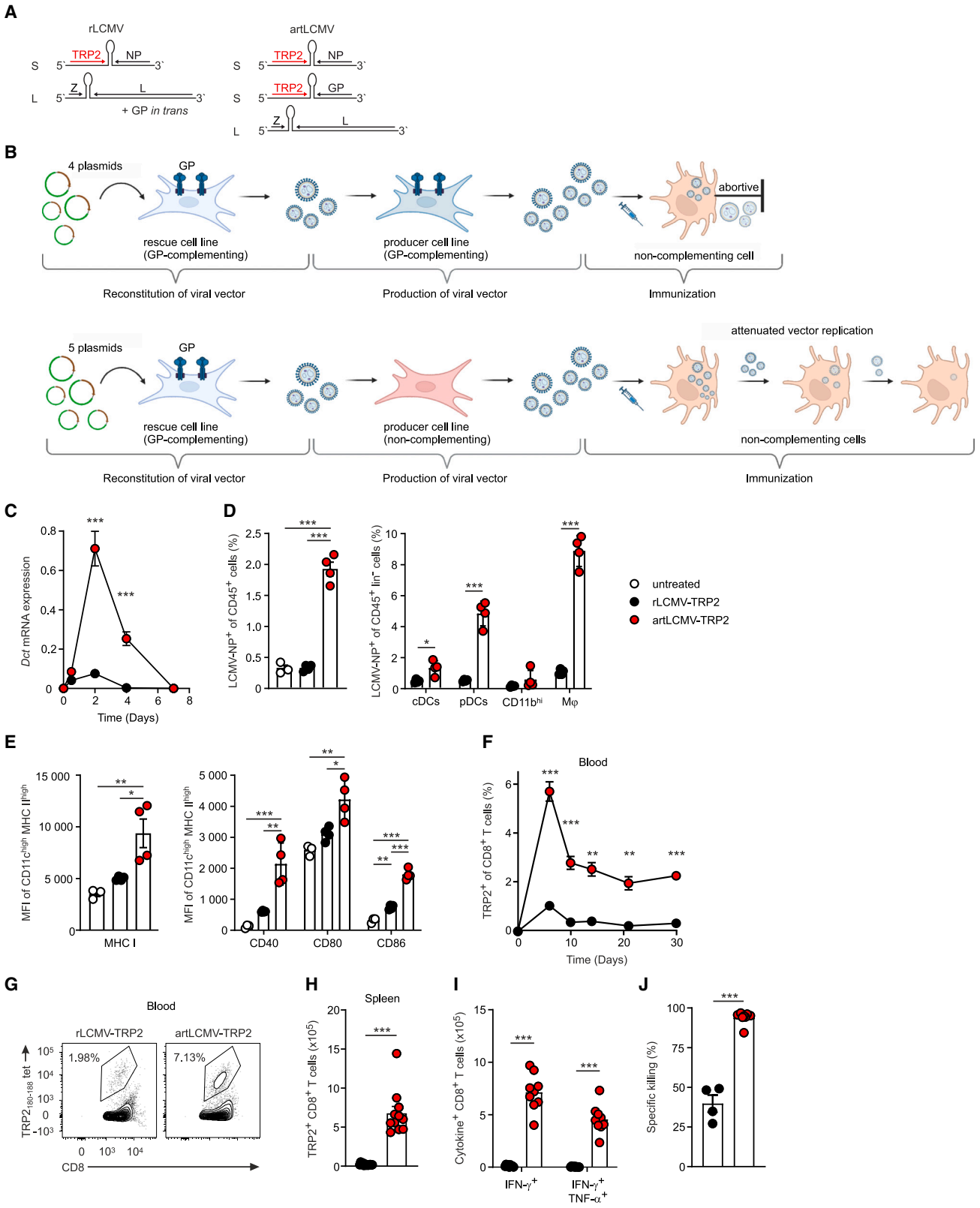

(legend on next page)

Please cite this article in press as: Purde et al., A replicating LCMV-based vaccine for the treatment of solid tumors, Molecular Therapy (2023), https://doi.org/10.1016/j.ymthe.2023.11.026

opposing challenges for the immunotherapy: it must overcome existing tolerance to the self-antigen being targeted while avoiding damage to the healthy tissues also expressing this molecule. Some patients with cancer already harbor a population of T cells recognizing tumor-associated and/or tumor-specific antigens, which can be unleashed therapeutically with the use of immune checkpoint inhibitors (ICIs). In these patients, ICIs can effectively prolong survival[3,4]; however, ICI treatment also unleashes other T cells with less desirable outcomes, often leading to severe and treatment-limiting autoimmune side effects.[5] Moreover, many patients, including those with non-inflamed tumors, do not respond to ICIs.[6] Thus, an effective immunotherapy must be able to overcome these obstacles to induce a durable, effective, and specific antitumor immune response across a diverse group of patients, including those lacking an existing T cell population recognizing the antigen of interest.

Virus-based vectors encoding tumor antigens are promising candidates for cancer immunotherapy, since they engage several steps of the cancer-immunity cycle. Lymphocytic choriomeningitis virus (LCMV) is a non-cytopathic arenavirus that mainly infects rodents, which has been a potent tool for studying T cell immunology for decades.[7] It efficiently generates cytotoxic T cell responses that provide long-lasting immunological memory.[8,9] Non-replicating LCMV-based vectors (rLCMVs) exhibit a great safety profile and can induce T cell and antibody responses against non-self antigens, such as viral antigens or the model antigen ovalbumin (OVA).[10–13] This makes rLCMV vectors promising therapeutic candidates for infectious disease indications.

However, targeting tumor-associated antigens poses additional challenges, such as the necessity to overcome tolerance and an often immunosuppressive tumor microenvironment. Preclinical studies have shown that replicating LCMV (artLCMV) vectors can possibly contribute to overcoming these challenges.[14,15] The potential of artLCMV vectors is further supported by promising results from a first-in-human phase I/II clinical trial that explored artLCMV vectors expressing the tumor-specific oncoproteins E6/E7 from human papillomavirus strain 16.[15,16] Nevertheless, the importance of prolonged vector persistence, the ability of such an approach to overcome tolerance to tumor-associated self-antigens, and the mechanisms leading to tumor control have yet to be determined.

Here, we systematically define the parameters of a successful LCMV-based cancer vaccine in a murine model of melanoma. We demonstrate that the ability to replicate and propagate is crucial in overcoming tolerance for the melanoma-associated self-antigen TRP2, and in inducing a strong *de novo* TRP2-specific $CD8^+$ T cell response that can successfully control the growth of established tumors. We further demonstrate the potential of combining the replicating viral vector with adoptive T cell transfer therapy, which leads to complete tumor rejection and reprogramming of the tumor microenvironment in our model.

RESULTS

Replication of the LCMV-based vector is required to overcome tolerance to a self-antigen

To investigate the mechanisms of action and parameters of success of LCMV-based cancer vaccines, as well as the different properties of non-replicating LCMV vectors (rLCMV) and replicating LCMV vectors (artLCMV), we chose to target the prototypic melanoma-associated antigen tyrosinase-related protein 2 (TRP2), which has high similarity in mice and humans.[17] The vaccines were constructed as two molecularly similar recombinant LCMV-based vectors carrying TRP2: the non-replicating rLCMV-TRP2 and the replicating, but attenuated, artLCMV-TRP2 (Figures 1A and 1B).[10,14] In contrast to the single-round infectious rLCMV viral particles, which lack the genomic information for the viral glycoprotein (GP) and thus need to be produced in GP-complementing cells,[18] replicating artLCMV vectors have been equipped with an additional genomic S segment that carries the GP open reading frame (ORF) under the control of the 3′ untranslated region. This artificial genomic setup (introduction of a third genomic segment and the GP ORF in an unnatural position) allows for self-limiting and attenuated vector replication in cells that do not complement LCMV GP.

Figure 1. Replication of the LCMV-based vector is required to overcome tolerance to a self-antigen

(A) Schematic of the recombinant LCMV vector genomes. The WT LCMV genome consists of the small (S) and large (L) segments. For the rLCMV vector, GP on the S segment is substituted with the full-length sequence of the melanoma-associated antigen TRP2. For artLCMV, GP is reintroduced on an additional S segment under the control of the 3′ UTR. (B) Schematic of the production and replication of the recombinant LCMV vectors. The rescue cells are transfected with plasmids encoding the viral S and L genome and two expression plasmids encoding the LCMV NP and polymerase. The GP-deficient rLCMV vector is produced in a GP-complementing cell line to provide GP for the first round of infections. All rLCMV particles newly synthesized in immunized cells are GP deficient, which renders the vector replication deficient. The artLCMV vector produces GP and is thus capable of replication. However, its replication is attenuated and it causes a self-limiting infection. Created with BioRender.com. (C–H) WT mice were immunized with rLCMV-TRP2 or artLCMV-TRP2. (C) Expression of *Dct* mRNA in spleens of immunized mice over time (n = 3, two-way ANOVA). (D) Infection of $CD45^+$ cells and transduction of APC subpopulations in the spleen at d4 (n = 3, two-tailed t tests with Holm-Šídák correction for multiple comparisons). (E) Surface expression levels of MHC I and T cell costimulatory molecules on $CD11c^{high}$ MHC II^{high} cDCs in immunized and unimmunized mice at d4 (n = 3, one-way ANOVA). (F–H) Frequency of TRP2-specific $CD8^+$ T cells (measured by $TRP2_{180\text{-}188}$-PE tetramer binding) in blood over time (F; n = 6, two-way ANOVA), in blood at d6 (G; representative flow cytometry plots), and in spleen at d6 after immunization (H; n = 11, two-tailed t test). (I) Frequency of cytokine-producing $CD8^+$ T cells from spleen after *ex vivo* restimulation with TRP2 peptides at d6 after immunization (n = 9, two-tailed t tests with Holm-Šídák correction for multiple comparisons). (J) Splenocytes from naive mice were pulsed with TRP2 peptides. A 1:1 mixture of pulsed and unpulsed cells labeled with different concentrations of CFSE was injected intravenously into mice immunized with rLCMV-TRP2 or artLCMV-TRP2. Specific *in vivo* killing of TRP2-pulsed target cells after 6 h (n = 4, two-tailed t test). APC, antigen-presenting cell; cDC, conventional dendritic cell; CFSE, carboxyfluorescein succinimidyl ester; GP, glycoprotein; Mφ, macrophage; NP, nucleoprotein; pDC, plasmacytoid dendritic cell; UTR, untranslated region. Summarized data with error bars depict mean ± SEM. Statistical significance: $^*p < 0.05$, $^{**}p < 0.01$, $^{***}p < 0.001$.

Please cite this article in press as: Purde et al., A replicating LCMV-based vaccine for the treatment of solid tumors, Molecular Therapy (2023), https://doi.org/10.1016/j.ymthe.2023.11.026

Overcoming tolerance to induce a T cell response to a tumor-associated self-antigen requires efficient and prolonged expression of the antigen and effective targeting of professional APCs.[1,19] Therefore, we measured the expression of *Dct*—the gene that encodes TRP2—in the spleens of immunized wild-type (WT) mice. We found that transcripts for the inserted antigen, TRP2, reached significantly higher levels and persisted longer in the spleens of mice immunized with artLCMV compared with rLCMV (Figure 1C). Mice immunized with artLCMV also demonstrated significantly higher frequencies of vector-infected immune ($CD45^+$) cells and, among those, a higher frequency of transduction of conventional dendritic cells (cDCs), plasmacytoid DCs, and macrophages (Figure 1D). Furthermore, expression levels of major histocompatibility complex (MHC) I ($H\text{-}2K^b$ and D^b) and costimulatory molecules CD40, CD80, and CD86 were significantly higher on $CD11c^{high}$ MHC II^{high} cDCs from mice immunized with artLCMV-TRP2, indicating a stronger activation of these cells (Figure 1E). The replicating artLCMV vector demonstrates an increased *in vivo* transduction efficiency of murine APCs in the spleen, longer persistence of the introduced antigen, and a more powerful activation of the innate immune system compared with rLCMV. Thus, the artLCMV vector efficiently engages the first steps of the cancer-immunity cycle.

We next asked whether a replicating virus-based vector could induce T cell responses against murine TRP2 and succeed in breaking tolerance to this self-antigen. We immunized mice with rLCMV-TRP2 or artLCMV-TRP2 and found that the replicating vector induced significantly higher frequencies and numbers of TRP2-specific $CD8^+$ T cells (referred to hereafter in the figures as $TRP2^+$ $CD8^+$ T cells) in blood (Figures 1F and 1G) and spleen (Figure 1H). After *ex vivo* restimulation of splenocytes with TRP2 peptides, a significantly higher frequency of $CD8^+$ T cells from artLCMV-immunized mice produced the effector cytokines interferon (IFN)-γ and tumor necrosis factor (TNF)-α (Figure 1I). Moreover, mice immunized with artLCMV-TRP2 demonstrated superior *in vivo* cytotoxicity against intravenously transferred TRP2-pulsed target cells compared with rLCMV-immunized mice (Figure 1J). These data suggest that active replication of the LCMV vector is a crucial factor allowing WT mice to overcome tolerance mechanisms against the tumor-associated self-antigen TRP2.

Immunization with a replicating vector promotes control of tumor growth

To assess whether immunization-induced TRP2-specific T cells could inhibit tumor growth, we immunized mice 7 days after subcutaneous or intravenous inoculation of B16F10 melanoma cells (Figure 2A). Immunization with artLCMV-TRP2 resulted in a significant delay of tumor growth in both the subcutaneous (Figure 2B) and the lung metastasis models (Figure 2C), compared with rLCMV-TRP2 immunization, which did not provide a detectable therapeutic benefit. To extend our findings to other melanoma models, we also tested artLCMV-TRP2 on the autochthonous 7,12-dimethylbenz[*a*]anthracene (DMBA) inducible primary melanoma model in $HgfxCdk4^{R24C}$ mice and on the slow-growing HCmel3 melanoma cell line derived from these mice.[20] The vector inhibited tumor growth and conferred a significant survival advantage compared with untreated mice (Figure S1).

We then generated a B16F10 cell line lacking the tumor antigen TRP2 (B16F10-$Dct^{-/-}$) to investigate the role of the adaptive immune response in mediating tumor control after immunization (see section "materials and methods"; Table S1; Figure S2). Tumor growth was comparable in untreated mice inoculated with B16F10 WT or B16F10-$Dct^{-/-}$ cell lines (Figure 2D). However, the antitumor efficacy of artLCMV-TRP2 immunization was largely abrogated in mice bearing B16F10-$Dct^{-/-}$ tumors compared with WT B16F10, suggesting that the adaptive immune response directed against TRP2 contributed to the antitumor response (Figure 2D). Collectively, our data show that tumor antigen TRP2-specific immune responses induced by the replicating artLCMV vector control tumor growth in different mouse melanoma models.

Additionally, we studied the responses to TRP2 as a tumor-specific "foreign" antigen, using TRP2 knockout (KO) mice lacking the *Dct* gene.[21] After immunization with rLCMV-TRP2, TRP2 KO mice showed a significantly higher frequency of TRP2-specific $CD8^+$ T cells than WT mice, in which TRP2 as a self-antigen would be subject to immune tolerance (Figures S3A and S3B). After *ex vivo* restimulation of splenocytes from immunized mice with TRP2 peptides, a greater proportion of the $CD8^+$ T cells from TRP2 KO mice produced effector cytokines compared with WT mice (Figure S3C). We assessed the therapeutic efficacy of rLCMV-TRP2 by immunizing KO and WT mice bearing palpable subcutaneous B16F10 tumors (Figure S3D). Immunization with rLCMV-TRP2 significantly delayed tumor growth and prolonged survival of TRP2 KO mice (Figure S3E). However, in WT mice, tumors grew as fast in immunized as in unimmunized mice (Figure S3F). These data show that the non-replicating rLCMV vector can induce potent immune responses to foreign but not self-antigens.

A replicating vector increases the ratio of $CD8^+$ effector to regulatory T cells

After infection with LCMV, innate sensing of pathogen-associated molecular patterns by APCs induces a strong type I IFN (IFN-α/β) response, which is crucial for the expansion of cytotoxic T cells.[22,23] Accordingly, we observed significantly higher concentrations of IFN-α in serum and spleen of WT mice immunized with artLCMV compared with rLCMV-immunized mice (Figure 3A). Blockade of the receptor for type I IFNs (IFN-α/β receptor 1, IFNAR1) in artLCMV-TRP2-treated animals also abolished tumor control (Figure 3B), suggesting that IFN-I is crucial for the generation of antitumor immune responses, consistent with previous work.[24]

Type I IFN has also been shown to inhibit the proliferation and activation of regulatory T cells (Tregs) in LCMV infections, thereby facilitating the generation of potent antiviral T cell responses.[25] Therefore, we assessed the influence of immunization with both recombinant LCMV vectors on Tregs and found transiently decreased frequencies

Please cite this article in press as: Purde et al., A replicating LCMV-based vaccine for the treatment of solid tumors, Molecular Therapy (2023), https://doi.org/10.1016/j.ymthe.2023.11.026

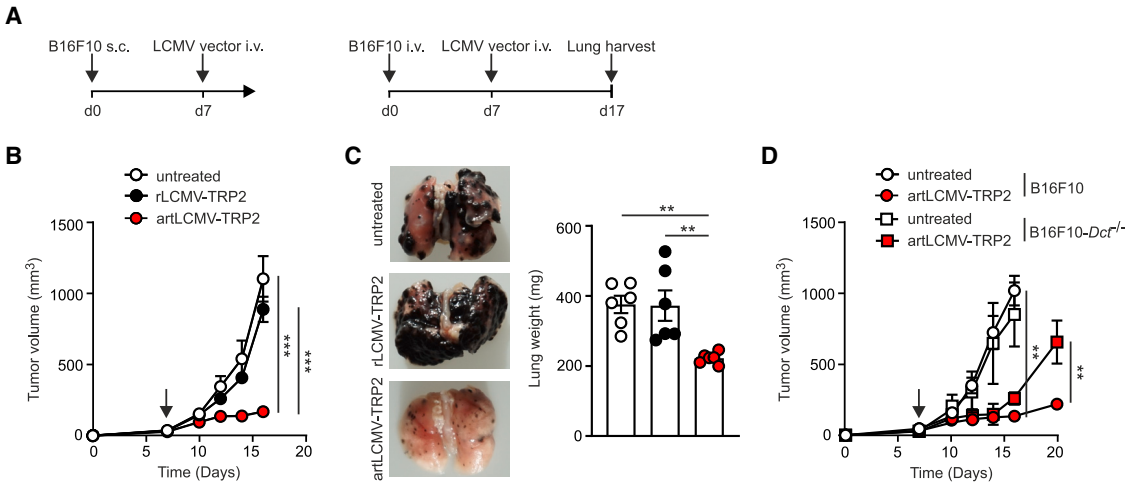

Figure 2. Immunization with a replicating vector promotes control of tumor growth

(A) Experimental setup of tumor growth experiments. WT mice were subcutaneously inoculated with B16F10 melanoma cells and intravenously immunized with rLCMV-TRP2 or artLCMV-TRP2 7 days later. In lung metastasis experiments, tumor cells were injected intravenously and lungs were harvested after 17 days. (B) Growth of subcutaneous tumors in immunized and unimmunized mice (n = 7, two-way ANOVA). Arrow indicates time point of immunization. (C) Growth of lung metastases in immunized and unimmunized mice, with representative images (n = 6, one-way ANOVA). (D) Growth of WT and TRP2-deficient (B16F10-*Dct*$^{-/-}$) tumors in immunized and unimmunized mice (n = 4, two-way ANOVA). See also Figures S1 and S2. Summarized data with error bars depict mean ± SEM. Statistical significance: *p < 0.05, **p < 0.01, ***p < 0.001.

and numbers of Tregs in the blood of both groups of immunized mice (Figure 3C). The decrease in Tregs began around the peak frequency of CD8$^+$ T cells, on day 6 post-immunization (Figure 1F), and appeared more pronounced in mice immunized with artLCMV-TRP2 compared with rLCMV-TRP2 (Figure 3C). The ratio of TRP2-specific CD8$^+$ T cells to Tregs was significantly higher in both blood and spleen after artLCMV immunization compared with rLCMV immunization (Figure 3D). Most notably, we found decreased frequencies and numbers of Tregs in the tumors of mice immunized with artLCMV compared with those of untreated and rLCMV-immunized mice (Figure 3E). Moreover, the TRP2$^+$CD8$^+$/Treg ratio was significantly higher in the tumors of artLCMV-immunized mice (Figure 3F). These findings suggest that the frequency of Tregs is transiently decreased in artLCMV-treated mice, thereby modulating the ratio of effector to regulatory T cells to allow the optimal expansion of self-antigen-specific CD8$^+$ T cells.

Immunization with a replicating vector induces abundant tumor infiltration

Efficacious immunotherapy relies on tumor-specific T cells infiltrating the tumor and executing their effector functions there.[26,27] To unravel the immunological changes inside the tumors of TRP2-vector-immunized mice, we harvested melanomas 7 days after immunization (day 14 after tumor implantation) and assessed immune infiltrates by flow cytometry. Notably, tumors from untreated mice showed little evidence of immune cell infiltration, while mice immunized with artLCMV showed a significantly higher density of tumor-infiltrating CD45$^+$ cells compared with both rLCMV-immunized and untreated mice (Figure 4A). Detailed analysis showed that approximately 80% of the tumor-infiltrating CD45$^+$ cells in artLCMV-TRP2-treated mice were CD8$^+$ T cells (Figure 4B). Compared with rLCMV-treated mice, the tumor-infiltrating T cells of artLCMV-immunized mice showed higher frequencies of CD8$^+$ and lower frequencies of CD4$^+$ T cells (Figure 4B). Despite this, the overall density of both CD8$^+$ and CD4$^+$ T cells was higher in tumors of artLCMV-immunized mice (Figures 4C and 4D).

Tetramer staining demonstrated high numbers of TRP2-specific CD8$^+$ T cells infiltrating the tumors of artLCMV-immunized mice (Figure 4E). Moreover, after *ex vivo* restimulation with TRP2 peptides, more of the tumor-infiltrating CD8$^+$ T cells in mice immunized with artLCMV-TRP2 demonstrated production of effector cytokines (Figure 4F), indicating greater functionality of TRP2-specific tumor-infiltrating lymphocytes (TILs) in those mice. We also assessed the likely functionality of the infiltrating T cells, as exhaustion of effector T cells is an additional hurdle for therapies that succeed in inducing tumor infiltration.[28] The tumor-infiltrating CD8$^+$ T cells from mice immunized with artLCMV-TRP2 showed a lower surface coexpression of exhaustion markers programmed cell death protein 1 (PD-1) and Tim-3 compared with rLCMV-immunized and untreated mice (Figure 4G). Overall, these data show that immunization with artLCMV-TRP2 induces extensive tumor infiltration by immune cells, particularly TRP2-specific CD8$^+$ T cells, which remain functional inside the tumor.

Immunization with a replicating vector induces complete tumor rejection in an adoptive cell transfer model

Adoptive cell transfer (ACT) of TILs or T cell receptor (TCR) engineered T cells, whereby high levels of tumor-specific T cells can be generated independently of the patient's natural repertoire

Please cite this article in press as: Purde et al., A replicating LCMV-based vaccine for the treatment of solid tumors, Molecular Therapy (2023), https://doi.org/10.1016/j.ymthe.2023.11.026

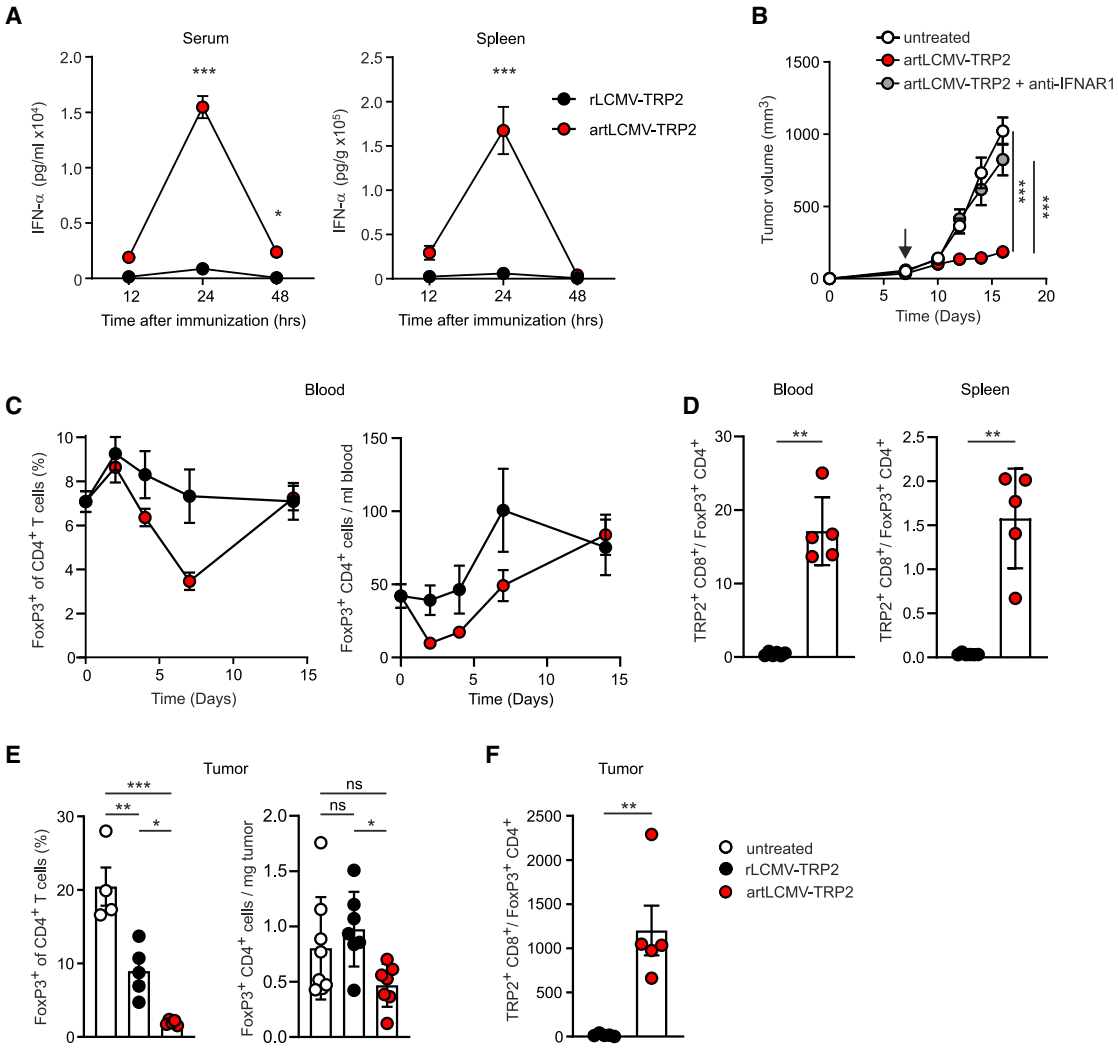

Figure 3. A replicating vector increases the ratio of CD8⁺ effector to regulatory T cells

WT mice were immunized with rLCMV-TRP2 or artLCMV-TRP2. (A) IFN-α level in serum and spleen of immunized mice (n = 3, two-way ANOVA). (B) Tumor growth in unimmunized mice, artLCMV-TRP2-immunized mice, and artLCMV-TRP2-immunized mice treated with IFNAR1-blocking antibodies (n = 5, two-way ANOVA). Arrow indicates time point of immunization. (C) Frequency and absolute number of Tregs in blood of immunized mice over time (n = 6, two-way ANOVA). (D) Ratio of TRP2-specific CD8⁺ T cells (measured by $TRP2_{180-188}$-PE tetramer binding) to Tregs in blood and spleen of immunized mice at d7 (n = 5, two-tailed t test). (E) Frequency and density of Tregs in tumors of immunized and unimmunized mice at d7 after immunization (n = 4, one-way ANOVA). (F) Ratio of TRP2-specific CD8⁺ T cells to Tregs in tumors of immunized mice (n = 5, two-tailed t test). IFNAR1, IFN-α/β receptor 1. Summarized data with error bars depict mean ± SEM. Statistical significance: *p < 0.05, **p < 0.01, ***p < 0.001.

composition, are promising emerging immunotherapy avenues.[29,30] However, the transferred cells do not become activated or expand optimally, leading to the need for administration of exogenous systemic interleukin (IL)-2.[29] We hypothesized that the high level of activation of antigen-specific effector T cells seen in immunized mice might extend to an ability of the two LCMV-based vectors to activate and expand transferred tumor-specific T cells. To test this, we administered tumor-bearing mice a transfer of naive TRP2-specific CD8⁺ T cells from TRP2 TCR transgenic mice concurrent with immunization at day 7 (Figure 5A). Mice immunized with rLCMV-TRP2 showed a temporary reduction in tumor size, whereas mice receiving artLCMV-TRP2 demonstrated complete tumor rejection and long-term survival (Figure 5B). ArtLCMV-immunized mice also developed local (at the site of the tumor) or generalized vitiligo, which was not seen in rLCMV-immunized mice or in any other experiments (Figure S4).

To study the composition of tumor-infiltrating immune cells in these mice, the tumors were harvested at day 15 (8 days after T cell transfer and immunization; Figure 5A) and analyzed using PhenoCycler (formerly CODEX),[31] a highly multiplexed immunofluorescence method (representative images in Figure 5C; reagents in Tables S2

Please cite this article in press as: Purde et al., A replicating LCMV-based vaccine for the treatment of solid tumors, Molecular Therapy (2023), https://doi.org/10.1016/j.ymthe.2023.11.026

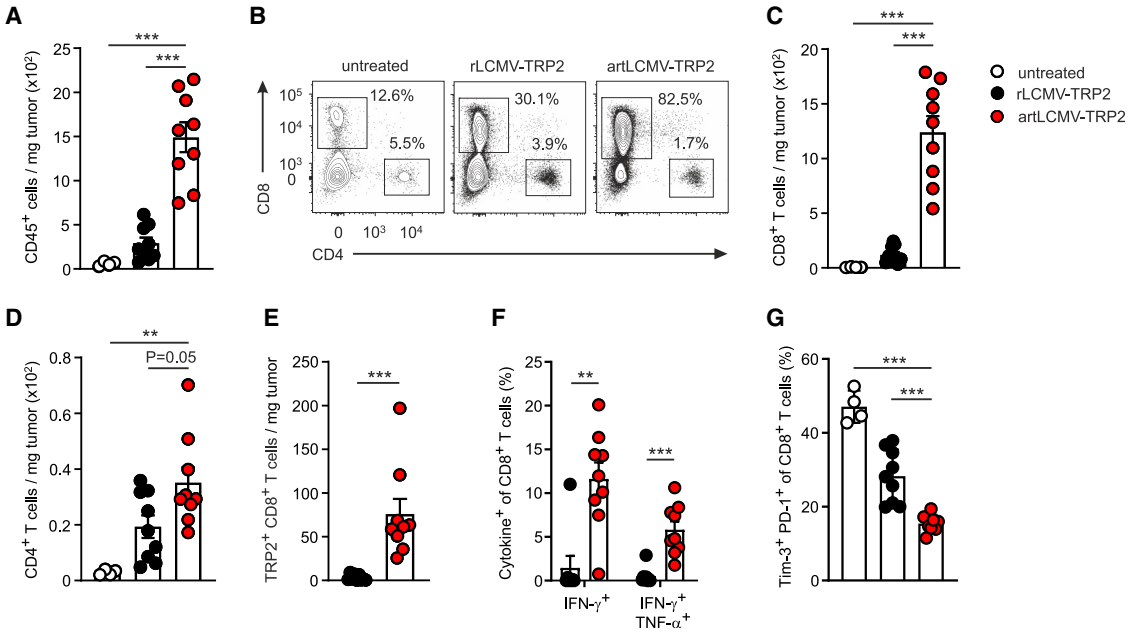

Figure 4. Immunization with a replicating vector induces abundant tumor infiltration

Tumors were harvested 14 days after implantation (7 days after immunization with rLCMV-TRP2 or artLCMV-TRP2). (A) Density of tumor-infiltrating CD45$^+$ cells (n = 4, one-way ANOVA). (B) Representative flow cytometry plots showing frequencies of CD8$^+$ and CD4$^+$ T cells in tumors from immunized and unimmunized mice. (C and D) Density of tumor-infiltrating CD8$^+$ (C; n = 4, one-way ANOVA) and CD4$^+$ (D; n = 4, one-way ANOVA) T cells. (E) Density of tumor-infiltrating TRP2-specific CD8$^+$ T cells (measured by TRP2$_{180\text{-}188}$-PE tetramer binding) in immunized mice (n = 9, two-tailed t test). (F) Frequency of cytokine-producing CD8$^+$ T cells from tumor after restimulation with TRP2 peptides *ex vivo* (n = 9, two-tailed t tests with Holm-Šídák correction for multiple comparisons). (G) Surface expression levels of exhaustion markers Tim-3 and PD-1 on tumor-infiltrating CD8$^+$ T cells (n = 4, one-way ANOVA). Summarized data with error bars depict mean ± SEM. Statistical significance: *p < 0.05, **p < 0.01, ***p < 0.001.

and S3). Cell types were identified using manual gating, similar to flow cytometry. Corroborating the data shown in Figure 4, we found increased immune infiltration in the tumors of artLCMV-immunized mice in the ACT setting (Figure 5D). As in Figure 4B, the tumor-infiltrating T cell compartment was skewed toward more CD8$^+$ and fewer CD4$^+$ T cells in artLCMV-immunized compared with rLCMV-immunized mice (Figure 5E). The tumors of artLCMV-immunized mice demonstrated significantly more infiltration of adoptively transferred CD8$^+$ T cells bearing the congenic marker CD90.1 (Figure 5F), indicative of greater proliferation and/or infiltration of transferred cells in those mice. The CD90.1$^+$ CD8$^+$ TILs also showed lower surface expression levels of the exhaustion marker PD-1 in mice immunized with artLCMV-TRP2 compared with rLCMV-TRP2 (Figure 5G).

For other analyses, cell types were also determined using unsupervised clustering (heatmap of markers and identified cell types in Figure S5A). Both methods identified similar numbers of cells (Figure S5B), validating the manual gating strategy. We again observed more infiltration of various immune cells, including CD8$^+$ T cells, in the tumors of artLCMV-immunized mice compared with rLCMV-immunized mice (representative images in Figure S5C). These data demonstrate the potential of combination therapy with a replicating virus-based vector and adoptive T cell transfer, which induces effective tumor control by tumor-infiltrating, self-antigen-specific CD8$^+$ T cells.

Immunization with a replicating vector supports proliferation of adoptively transferred T cells

To further investigate the fate of the adoptively transferred T cells, we transferred naive TRP2-specific CD8$^+$ T cells labeled with carboxyfluorescein succinimidyl ester (CFSE) concurrently with immunization. We then collected blood from recipient mice at 1, 2, and 3 days after transfer. At day 3, we observed a significant increase in the frequency of the transferred CD90.1$^+$ CD8$^+$ T cells in immunized compared with unimmunized mice (Figure 6A). Simultaneously, the mean fluorescence intensity of CFSE significantly decreased in those cells (Figure 6B), indicating proliferation of this cell population. The frequency of transferred CD8$^+$ T cells was significantly higher in the spleens of immunized compared with unimmunized mice at day 3, while we observed no significant difference between mice immunized with rLCMV-TRP2 and artLCMV-TRP2 (Figure 6C). However, at day 8 after ACT and immunization, artLCMV-immunized mice showed significantly higher frequencies of transferred CD8$^+$ T cells in the spleen (Figure 6D). This implies that the expansion of the transferred T cells is uninhibited in mice immunized with the replicating artLCMV vector.

DISCUSSION

To date, preventive cancer vaccines have been successful in reducing the incidence of virus-driven tumors, including cervical cancer and hepatocellular carcinoma.[32,33] In contrast, clinical trials targeting

Please cite this article in press as: Purde et al., A replicating LCMV-based vaccine for the treatment of solid tumors, Molecular Therapy (2023), https://doi.org/10.1016/j.ymthe.2023.11.026

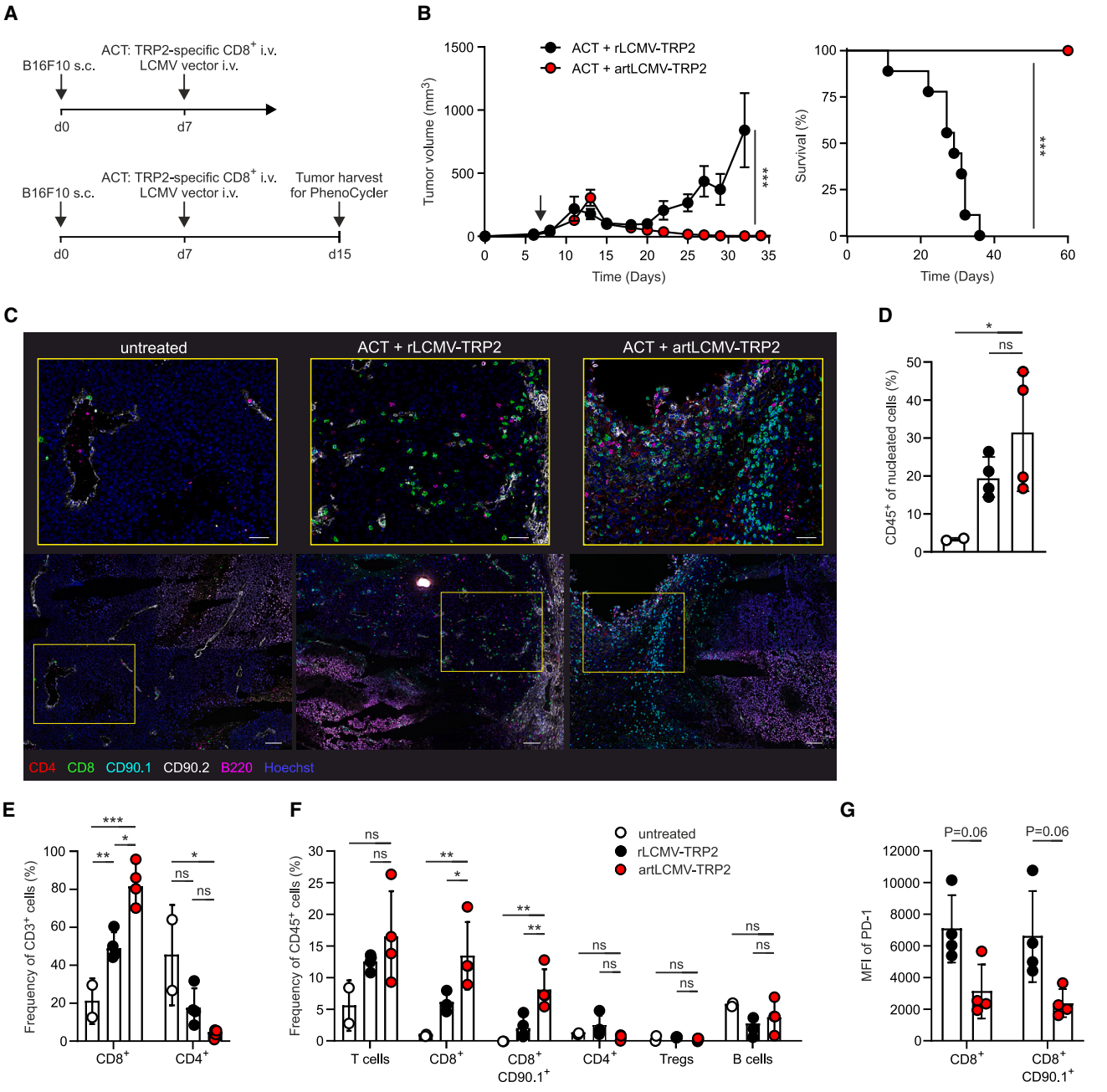

Figure 5. Immunization with a replicating vector induces complete tumor rejection in an ACT model

(A) Experimental setup of tumor growth experiments. B16F10 melanoma cells were injected subcutaneously into WT mice and, 7 days later, they were immunized intravenously with rLCMV-TRP2 or artLCMV-TRP2. Naive TRP2-specific CD8$^+$ T cells from TRP2 TCR transgenic mice were injected intravenously on the day of immunization. For the PhenoCycler assay, tumors were harvested 15 days after implantation (8 days after immunization). (B) Tumor growth and survival in mice receiving ACT and immunization (n = 9, two-way ANOVA and log rank test). Arrow indicates time point of immunization and ACT. (C) Representative images of selected markers in tumors of immunized and unimmunized mice. Scale bar, 50 μm for overview images and 25 μm for zoomed-in images. (D) Frequency of CD45$^+$ cells of nucleated cells in tumors of immunized and unimmunized mice (n = 4, one-way ANOVA). (E) Frequency of CD8$^+$ and CD4$^+$ T cells of total tumor-infiltrating T cells in immunized and unimmunized mice (n = 4, one-way ANOVA). (F) Frequency of various immune cell populations in tumors of immunized and unimmunized mice (n = 4, one-way ANOVA). (G) MFI of exhaustion marker PD-1 on total and transferred (CD90.1$^+$) tumor-infiltrating CD8$^+$ T cells in immunized mice (n = 6, two-tailed t tests with Holm-Šídák correction for multiple comparisons). ACT, adoptive cell transfer; MFI, mean fluorescence intensity; TCR, T cell receptor. See also Tables S2 and S3 and Figures S4 and S5. Summarized data with error bars depict mean ± SEM. Statistical significance: *p < 0.05, **p < 0.01, ***p < 0.001.

Please cite this article in press as: Purde et al., A replicating LCMV-based vaccine for the treatment of solid tumors, Molecular Therapy (2023), https://doi.org/10.1016/j.ymthe.2023.11.026

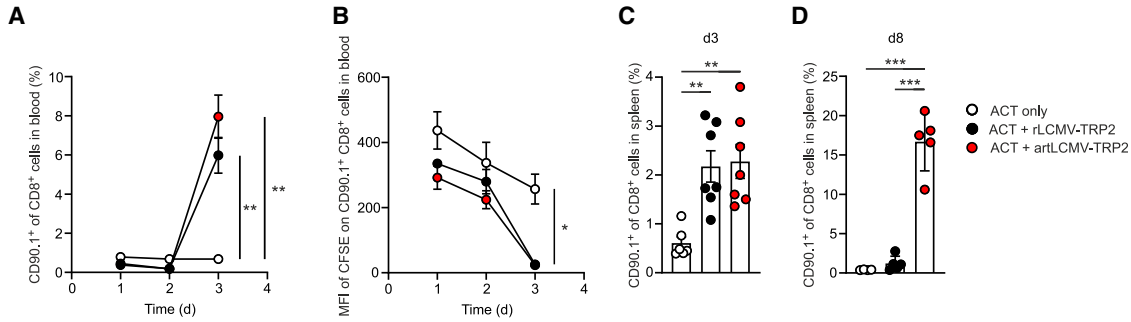

Figure 6. Immunization with a replicating vector supports proliferation of adoptively transferred T cells

WT mice received an adoptive transfer of naive TRP2-specific CD8$^+$ T cells from TRP2 TCR transgenic mice and were immunized with rLCMV-TRP2 or artLCMV-TRP2 on the same day. The transferred cells carried the congenic marker CD90.1 and were labeled with CFSE. (A) Frequency of transferred CD8$^+$ T cells in blood over time. (B) MFI of CFSE on transferred CD8$^+$ T cells in blood over time. (C) Frequency of transferred CD8$^+$ T cells in spleen 3 days after ACT and immunization. (D) Frequency of transferred CD8$^+$ T cells in spleen 8 days after ACT and immunization. Summarized data with error bars depict mean ± SEM. Statistical significance: *p < 0.05, **p < 0.01, ***p < 0.001.

self-antigens have shown modest success. Our study defines the features that are necessary for a successful self-antigen-targeting virus-based immunotherapy.

In contrast to ICIs or ACT, recombinant LCMV-based vectors interfere at several steps of the cancer-immunity cycle (graphical abstract).[1,34] In the context of viral replication, the self-antigen is delivered to professional APCs. Their activation results in increased expression of MHC I and the costimulatory molecules crucial for T cell priming. In addition, strong inflammatory signals such as IFN-I—induced by the virotherapy—enhance the responsiveness of cytotoxic T cells.[35] As we observed in mice inoculated with *Dct*-deficient tumor cells, the strong activation of innate immunity by the replicating artLCMV vector can temporarily delay tumor growth, even when the tumor does not express the vector antigen.

Type I IFN further serves as a signal for the expansion of tumor-specific CD8$^+$ T cells and decreases the frequency of regulatory T cells, thereby removing an important inhibitory mechanism.[25,36] Furthermore, immunization with the replicating vector induces tumor infiltration by self-antigen-specific T cells, leading to tumor cell killing and resulting in prolonged survival. Our data indicate that self-antigen persisting over an extended period is associated with overcoming tolerance mechanisms: immunization with artLCMV-TRP2 achieves this, driving the cancer-immunity cycle.

Cancer therapies frequently target tumor-associated self-antigens since those are shared between many patients, making the treatment widely applicable. Self-antigen-specific T cell responses have been found to correlate with immunotherapy response and overall survival.[37,38] The bispecific molecule tebentafusp, which targets the melanoma-associated antigen GP100, has demonstrated significant survival improvement in patients with metastatic uveal melanoma.[39] However, due to the MHC-restricted nature of antigen recognition by T cell receptors, this treatment is limited to patients carrying HLA-A*02:01.

Treatment with the patient's own TILs can mediate objective responses in metastatic melanoma but requires TIL presence and *ex vivo* expansion, as well as a cumbersome conditioning/lymphodepleting regime before reinfusion.[40,41] Thus, "off-the-shelf" virus-based vectors inducing endogenous tumor-specific T cells represent a desirable approach. An important advantage of this system is that the full-length protein sequence can be inserted into the vector, which allows the production of an HLA-independent therapy suitable for most patients. Here we have also demonstrated the synergistic interaction of vector immunization and adoptive T cell transfer. The replicating viral vector reprogrammed the tumor microenvironment from "cold" to "hot," stimulating the transferred cytotoxic T cells and various other immune cells to infiltrate the tumor, which led to complete tumor rejection. Importantly, the combination therapy was successful without prior lymphodepletion or administration of IL-2, which are standard regimens for adoptive T cell therapy, but can lead to adverse effects including infections and toxicities.[29,42,43]

In summary, this study uncovers the importance of replication of LCMV-based vectors for self-antigen-targeting cancer immunotherapies. Unlike the non-replicating rLCMV, replicating artLCMV vectors can overcome tolerance to self and induce a strong IFN-I response, which leads to a potent antitumor immunity mediated by self-antigen-specific cytotoxic T cells infiltrating the tumor. Moreover, combining artLCMV immunization with adoptive T cell transfer shows great potential as an avenue for effective cancer treatment.

MATERIALS AND METHODS

Study design

The objective of this study was to investigate the efficacy of replicating and non-replicating viral vectors as cancer vaccines targeting tumor-associated self-antigens. We employed various mouse strains and murine melanoma models to study the effects of immunization in different settings. We used flow cytometry, PhenoCycler, and ELISA to monitor the immune response following immunization in different tissue compartments. Experiments were performed at least

Please cite this article in press as: Purde et al., A replicating LCMV-based vaccine for the treatment of solid tumors, Molecular Therapy (2023), https://doi.org/10.1016/j.ymthe.2023.11.026

twice. All data points represent biological replicates. Statistical analyses are reported in each figure legend.

Cells and cell lines

B16F10 cells were obtained from ATCC (Manassas, VA) and cultured in complete Dulbecco's modified Eagle's medium (DMEM; Gibco, Thermo Fisher Scientific, Waltham, MA) supplemented with 10% (v/v) fetal calf serum (FCS; Capricorn Scientific, Ebsdorfergrund, Germany), 10 mmol/L non-essential amino acids (NEAAs; Gibco, Thermo Fisher Scientific), 1 mmol/L sodium pyruvate, and 100 IU/mL penicillin/streptomycin (Lonza, Basel, Switzerland). The HCmel3 cell line was cultured in RPMI-1640 (Sigma, Sigma-Aldrich, St. Louis, MO) containing 20% FCS, 2 mmol/L L-glutamine, 10 mmol/L NEAAs, 1 mmol/L HEPES, 20 μmol/L β-mercaptoethanol (Gibco, Thermo Fisher Scientific), and 100 IU/mL penicillin/streptomycin. BHK-21 and HEK293 cells were obtained from the Institute of Experimental Immunology, University of Zurich. All cell lines were kept at 37°C and 5% CO_2 in a humidified incubator and regularly examined for signs of mycoplasma infection.

Generation of the *Dct*-knockout B16F10 cell line

B16F10-*Dct*$^{-/-}$ cells were generated using CRISPR-Cas9 technology. Sequences for the single guide RNA (sgRNA; Table S1) were designed using the CHOPCHOP tool (available at http://chopchop.cbu.uib.no/index.php).[44,45] sgRNA was inserted into the pSpCas9(BB)-2A-GFP (PX458) plasmid (Addgene, 48138) expressing Cas9 and EGFP. B16F10 cells were transfected with the sgRNA PX458 plasmid targeting *Dct* (*Trp2*). The *Dct* gene from cells expressing GFP was amplified (primers shown in Table S1) and a T7 endonuclease I (T7EI) assay was performed to check genome-targeting efficiency. After subcloning, single clones were again tested for deletion of *Dct* using T7EI (Figure S2A). Sequencing (data not shown) and an intracellular flow cytometric analysis using an anti-TRP2 antibody (ab74073; Abcam, Cambridge, UK) confirmed the deletion of the *Dct* gene (Figure S2B). All cell lines were regularly tested for mycoplasma.

Recombinant vectors

Two different forms of LCMV-based vectors were constructed in this study: a replication-deficient bisegmented vector, rLCMV,[10] and a replicating trisegmented vector, artLCMV.[14] In both vectors, the viral GP on the small (S) segment is replaced with a target antigen: here, we inserted the full-length cDNA sequence of the murine melanoma-associated antigen TRP2. In the artLCMV vector, the viral GP is reintroduced under the control of the 3′ untranslated region of the second S segment, enabling the vector to replicate in host cells that do not complement LCMV nucleoprotein (NP) (Figure 1A). This genetic rearrangement further inhibits recombination of the two S segments and the generation of WT virus particles.

Both rLCMV and artLCMV vectors were generated by transient transfection of BHK-21 cells stably expressing the LCMV GP as described (Figure 1B).[46] Briefly, the cells were transfected with plasmids encoding the viral S and L genome segments and two expression plasmids encoding the LCMV NP and polymerase (L). To generate FCS-free vector stock material, suspension HEK293 cells either expressing the viral GP (for rLCMV) or not (for artLCMV) were infected at an MOI of 0.001 and incubated for 72 h while shaking. The cells were then propagated and incubated for another 2 days. Virus-containing supernatant was harvested after centrifugation of the cells and the infectious titer was determined by focus-forming assay (FFA) on either LCMV GP-complementing cells (focus-forming units, FFU) or non-complementing HEK293 cells (RCV FFU).[10,14] Briefly, monolayers of adherent HEK293-GP or HEK293 seeded in 24-well plates were infected with serial dilutions of the virus, incubated for 48 h, and subsequently fixed and stained with anti-NP antibody (VL-4; Bio X Cell, Lebanon, NH). The number of foci (clusters of infected cells) was determined and the virus titer was calculated.

Mice

C57BL/6N (B6) mice were obtained from Charles River Laboratories (Freiburg im Breisgau, Germany). *Hgf*x*Cdk4*^{R24C} (provided by Thomas Tüting, University of Bonn, Germany) were bred as previously described.[47] *Dct*$^{-/-}$ (TRP2 KO) mice were bred as previously described.[21] TRP2 TCR transgenic mice (provided by Andrea Schietinger, Memorial Sloan Kettering Cancer Center, New York, NY) were bred as previously described.[48] All mice were kept under specific-pathogen-free conditions in individually ventilated cages in a 12/12-h light/dark cycle. The mice were housed at a maximum density of six mice per cage, with aspen wood chips (SAFE aspen; SAFE, Rosenberg, Germany) as bedding and paper tissues for enrichment. Food (3436 mouse and rat maintenance extrudate; Kliba Nafag, Kaiseraugst, Switzerland) and water were provided *ad libitum*. All materials (cages, bedding, food, water bottles) were autoclaved before use.

For experiments, sex- and age-matched mice between 7 and 10 weeks of age were used. Experiments were performed in accordance with federal and cantonal guidelines (Tierschutzgesetz) under permission numbers SG02/14, SG01/16, SG03/18, SG01/20, SG04/20, SG/07/2021, and SG/03/2022 following review and approval by the respective Cantonal Veterinary Offices (St. Gallen and Berne, Switzerland).

Tumor graft models and immunization

To establish tumors in mice, 2×10^5 B16F10 or 4×10^5 HCmel3 melanoma cells in phosphate-buffered saline (PBS) were injected either subcutaneously into the flank or intravenously for the lung metastasis model. Primary melanomas in *Hgf*x*Cdk4*^{R24C} mice were induced by applying 100 nmol DMBA in acetone onto the shaved back.[20] When transplanted or primary tumors became palpable (20–50 mm^3), mice were treated with 1×10^6 FFU rLCMV-TRP2 or 1×10^5 RCV FFU artLCMV-TRP2 in PBS injected intravenously. The size of subcutaneous tumors was measured with calipers two or three times per week. Tumor volume was calculated as $width^2 \times length \times 0.5$.[49,50] Mice were sacrificed when tumor size exceeded 1,000 mm^3 or upon showing signs of illness. In the lung metastasis model, mice were sacrificed and lungs were harvested at day 17 of tumor growth.

Please cite this article in press as: Purde et al., A replicating LCMV-based vaccine for the treatment of solid tumors, Molecular Therapy (2023), https://doi.org/10.1016/j.ymthe.2023.11.026

For *in vivo* blockade of the type I IFN receptor, anti-IFNAR1 (clone MAR1-5A3, BE0241; Bio X Cell, Lebanon, NH) in PBS was injected intraperitoneally into mice, with 1 mg 1 day before immunization and with 250 μg on days 2 and 5 after immunization.

Tissue processing and flow cytometry

For the generation of single-cell suspensions, spleens were collected into RPMI-1640 supplemented with 5% FCS and mechanically disrupted on a 70-μm pore size cell strainer (Falcon, Corning, New York, NY). To isolate tumor-infiltrating immune cells, tumors were separated from the surrounding skin and then dissociated using scissors and a syringe plunger. Cells were passed through a 70-μm pore size cell strainer and washed once before density-gradient (Lympholyte-M; Cedarlane, Burlington, Canada) centrifugation to allow collection of immune cells at the interface. Blood was collected into PBS containing 0.5% FCS and 10 mmol/L EDTA, and erythrocytes were lysed using the BD Lysing solution (BD Biosciences, Franklin Lakes, NJ).

For flow cytometry, single-cell suspensions were stained with Zombie Aqua in PBS according to the manufacturer's instructions (Zombie Aqua Fixable Viability Kit; BioLegend, San Diego, CA) to discriminate between live and dead cells. For identification of epitope-specific T cells, cells were incubated with PE-labeled H-2K^b-TRP2$_{180\text{-}188}$ tetramer (MBL, JSR Life Sciences, Sunnyvale, CA) or PE-labeled H-2D^b-LCMV-NP$_{396\text{-}404}$ tetramer (NIH Tetramer Core Facility, Emory University, Atlanta, GA) for 10 min at 37°C. For detection of surface molecules, cells were incubated for 20 min at 4°C in PBS containing 0.5% FCS and 10 mmol/L EDTA with the indicated antibodies (Table S4). For intracellular or intranuclear labeling or staining, cells were fixed and permeabilized using the BD Cytofix/Cytoperm (BD Biosciences) or the FoxP3 Transcription Factor staining kits (eBioscience, Thermo Fisher Scientific). Data were acquired with a BD LSR Fortessa (BD Biosciences) and data analysis was performed using FlowJo (FlowJo, BD Biosciences).

Ex vivo restimulation and cytokine production

For the assessment of *ex vivo* cytokine secretion, lymphocytes were resuspended in RPMI-1640 containing 5% FCS and 0.4% β-mercaptoethanol and incubated with 1 μM concentration of the TRP2$_{180\text{-}188}$ peptide (SVYDFFVWL; GenScript, Piscataway, NJ) in the presence of 10 μg/mL brefeldin A (Sigma-Aldrich) for 5 h at 37°C. The frequency of IFN-γ- and TNF-α-producing cells was determined by subtracting the medium (no-peptide) control.

ACT

Spleens from unimmunized TRP2 TCR transgenic mice were collected and dissociated as described above to obtain a single-cell suspension. The cells were treated with erythrocyte lysis buffer (water, 0.15 M NH_4Cl, 1 mM $KHCO_3$, 0.1 mM EDTA; 1 mL per spleen) at room temperature (RT) for 3 min and washed with ice-cold PBS. If the cell pellet was red after centrifugation, the lysis step was repeated. If tracing of the transferred cells was required, cells were labeled with CFSE (CellTrace CFSE Proliferation Kit, Life Technologies, Thermo Fisher Scientific) according to the manufacturer's instructions. A sample of the splenocytes was stained with the H-2K^b-TRP2$_{180\text{-}188}$ tetramer and antibodies against surface markers as described above to determine the frequency of TRP2-specific CD8$^+$ T cells. Total cell number was counted using a hemocytometer and the splenocytes were administered intravenously at 5×10^5 TRP2-specific CD8$^+$ T cells per recipient.

PhenoCycler staining and imaging

For the PhenoCycler assay, B16F10 melanoma cells were subcutaneously inoculated into mice, which were then immunized as above. Tumors from rLCMV-TRP2-immunized, artLCMV-TRP2-immunized, and unimmunized WT mice were harvested at day 15 and fresh frozen (FF) in frozen section embedding medium (FSC 22 Clear; Surgipath, Leica Biosystems, Wetzlar, Germany). PhenoCycler imaging was performed as previously described.[31,51–53] All steps were performed at RT unless indicated otherwise. Briefly, FF tumors were assembled into tissue arrays and sectioned on a cryostat (Leica). Sections 7 μm thick were placed on 22 × 22-mm glass coverslips (#1.5; Electron Microscopy Sciences, Hatfield, PA) pre-coated with poly-L-lysine (Sigma, Sigma-Aldrich), air-dried, and stored at −80°C.

For staining, tissue sections on coverslips were removed from the freezer, dried on indicating desiccant (Drierite; Thermo Fisher Scientific) for 2 min, fixed in acetone for 10 min, and dried in a humidity chamber for 2 min. Tissues were rehydrated in buffer S1 for 2 min twice in separate wells of a six-well plate, fixed with 1.6% paraformaldehyde (PFA; Thermo Fisher Scientific) in buffer S1 for 10 min, washed twice in buffer S1, and equilibrated in blocking buffer for 30 min.

The antibody cocktail (Table S2) was prepared in buffer S2 containing 0.065 mg/mL mouse immunoglobulin (Ig) G (Biozol, Eching, Germany), 0.065 mg/mL rat IgG (Biozol), 0.43 mg/mL sheared salmon sperm DNA (Invitrogen, Thermo Fisher Scientific), and a mixture of non-fluorescent PhenoCycler oligonucleotides (Integrated DNA Technologies, Coralville, IA) at a final concentration of 0.5 mM. Staining was performed in 100 μL of this cocktail for 3 h in a humidity chamber. Tissues were then washed twice in buffer S2, fixed with 1.6% PFA in buffer S4 for 10 min, washed thrice in PBS, fixed with ice-cold methanol for 5 min, washed thrice in PBS, fixed with 3 mg/mL BS^3 fixative (Thermo Fisher Scientific) in PBS for 20 min, and washed again thrice in PBS. The coverslips were stored in buffer S4 until imaging.

Coverslips were placed onto the stage of the PhenoCycler (Akoya Biosciences, Marlborough, MA). Nuclei were stained with Hoechst nuclear stain (Thermo Fisher Scientific) diluted 1:1,000 in buffer H2 for 1 min, followed by washing thrice with buffer H2. Imaging was performed on an inverted fluorescence microscope (BZ-X810; Keyence, Osaka, Japan) according to the manufacturer's instructions (Akoya Biosciences).

PhenoCycler image processing and data analysis

At least one 1,920 × 1,440-μm region was selected on each tissue sample. If possible, two regions were selected; however, some tumors were too small or had large necrotic areas. Images were processed and segmented using the CRISP-CODEX-Processor-main and CellSeg-CRISP-master packages.[54] After quality control using the ImageJ/Fiji software, the flow cytometry standard (.fcs) files resulting from the segmentation were analyzed using CellEngine cytometry analysis software (manual gating; https://cellengine.com; CellCarta, Montreal, Canada). For Figure 5, values from regions of the same tissue were averaged so as not to bias the results toward the larger tissue samples. Fluorescence microscopy overlay images were created using ImageJ/Fiji software and custom scripts.

Single-cell staining intensity data across all regions were stored in Microsoft Excel (Microsoft, Redmond, WA) as comma-separated values (.csv) files, which were concatenated together and analyzed as a single dataset using HFcluster.[54] Unsupervised clustering yielded 49 primary clusters, which were subjected to manual annotation guided by the anticipated antibody staining patterns. This culminated in the identification of nine distinct cell subsets (Figure S5A), each of which was rigorously validated against the original image data to ensure the accuracy and fidelity of the annotations. Subsequently, the identified cells were superimposed onto the tissue. Correlations between cell counts of identical cell types identified by manual gating and by clustering were established using Prism (GraphPad Software, Boston, MA).

In vivo cytotoxicity assay

Mice were immunized with rLCMV- or artLCMV-TRP2 and received TRP2-pulsed target cells 7 days after the immunization. Briefly, single-cell splenocyte suspensions were subjected to erythrocyte lysis by osmotic shock. Splenocytes were incubated with 10^{-6} M $TRP2_{180\text{-}188}$ peptide for 1.5 h at 37°C (pulsed) or left untreated (unpulsed). Cells were labeled using 10 μL of 5 mM CFSE ($CFSE^{high}$; pulsed) or 0.5 mM CFSE ($CFSE^{low}$; unpulsed) according to the manufacturer's protocol. Pulsed $CFSE^{high}$ and unpulsed $CFSE^{low}$ splenocytes were mixed at a 1:1 ratio, and 2×10^7 cells were injected intravenously into mice immunized with rLCMV-TRP2 or artLCMV-TRP2. Six hours after transfer, the presence of $CFSE^{high}$ (pulsed) and $CFSE^{low}$ (unpulsed) cells in blood was analyzed and specific killing was calculated using the following formula:[55]

$$100 - \left(\frac{\%\ pulsed\ in\ infected}{\%\ unpulsed\ in\ infected} \div \frac{\%\ pulsed\ in\ uninfected}{\%\ unpulsed\ in\ uninfected} \times 100 \right)$$

Quantitative real-time PCR

Total mRNA was extracted from the spleen by TRIzol (Ambion, Thermo Fisher Scientific) using the Direct-zol RNA Kit (ZYMO Research, Irvine, CA) and cDNA was generated using the QuantiTect Reverse Transcription Kit (Qiagen, Hilden, Germany). TRP2 and TATA binding protein (TBP) were amplified by qRT-PCR using the SYBR Green Master Mix (Applied Biosystems, Thermo Fisher Scientific). The primers are listed in Table S5. For analysis, the expression levels of the target gene TRP2 were normalized to TBP mRNA expression. Relative gene expression levels were calculated with the ΔC_T method.[56]

IFN-α ELISA

Levels of IFN-α in serum were determined using the mouse IFN-α ELISA kit according to the manufacturer's instructions (Genprice Research Diagnostics, Baileys Harbor, WI).

Statistical analysis

Statistical analysis was performed using Prism 9.4.1 (GraphPad Software, Boston, MA). Unless specified otherwise, graphs depict mean ± standard error. Differences between two groups were evaluated using an unpaired two-tailed Student's t test followed by Holm-Šídák correction for multiple comparisons, if appropriate. Single values of multiple groups were compared by one- or two-way ANOVA followed by Bonferroni *post hoc* test. Kaplan-Meier survival curves were assessed using log rank tests. Results were considered statistically significant as follows: $^*p < 0.05$, $^{**}p < 0.01$, or $^{***}p < 0.001$.

DATA AND CODE AVAILABILITY

The authors declare that all data supporting the findings of this study are available within the article and its supplemental files or are available from the authors upon request.

SUPPLEMENTAL INFORMATION

Supplemental information can be found online at https://doi.org/10.1016/j.ymthe.2023.11.026.

ACKNOWLEDGMENTS

We thank Sonja Caviezel-Firner and Céline Engetschwiler (Institute of Immunobiology, Kantonsspital St. Gallen) and Christine Beschorner and Karen Greif (Department of Pathology, University Hospital Tübingen) for excellent technical support; Lucy Robinson (Insight Editing London) for outstanding writing and editing support; and Timo Schippers (Hookipa Pharma) for providing Figure 1B.
This study was funded by a Swiss National Science Foundation (SNSF) Professorship to L.F. (PP00P3_157448) and a grant from Hookipa Pharma. Work in the laboratory of C.M.S. was supported by core funding from the Department of Pathology, University Hospital Tübingen. L.B. was supported by the grant LX22NPO5102—Funded by the European Union—Next Generation EU. The funders had no role in study design, data collection and analysis, decision to publish, or preparation of the manuscript.

AUTHOR CONTRIBUTIONS

L.F. and S.S.R. designed the study. L.F. and C.M.S. provided funding and supervision. S.S.R., M.T.P., Y.A.P., A.M., F.H., A.L., M.T.A., and L.B. performed experiments and analyzed and discussed data. M.T.P., S.S.R., L.F., Y.A.P., and S.S. wrote the paper. S.S., F.S., T.T., S.K., B.L., H.L., K.K.O., A.S., and C.M.S. provided resources and discussed data. J.C., A.R., D.B., F.B., M.H., A.B., and T.B. discussed data.

DECLARATION OF INTERESTS

C.M.S. is a scientific advisor to, has stock options in, and has received research funding from Enable Medicine, Inc. L.F. is a founder and shareholder of Hookipa Pharma Inc. F.S., S.S., and K.K.O. are employees and stock option holder of Hookipa Pharma, Inc. L.F., S.S.R., S.S., and K.K.O. are listed as inventors of the patent entitled "Arenavirus particles to treat solid tumors" (patent number WO2018/185307 A1) describing the application of artLCMV vectors in the treatment of tumors.

REFERENCES

1. Chen, D.S., and Mellman, I. (2013). Oncology meets immunology: the cancer-immunity cycle. Immunity *39*, 1–10.
2. Kim, J.M., and Chen, D.S. (2016). Immune escape to PD-L1/PD-1 blockade: seven steps to success (or failure). Ann. Oncol. *27*, 1492–1504.
3. Liu, F.X., Ou, W., Diede, S.J., and Whitman, E.D. (2019). Real-world experience with pembrolizumab in patients with advanced melanoma: A large retrospective observational study. Medicine (Baltimore) *98*, e16542.
4. Huang, Z., Su, W., Lu, T., Wang, Y., Dong, Y., Qin, Y., Liu, D., Sun, L., and Jiao, W. (2020). First-Line Immune-Checkpoint Inhibitors in Non-Small Cell Lung Cancer: Current Landscape and Future Progress. Front. Pharmacol. *11*, 578091.
5. Albandar, H.J., Fuqua, J., Albandar, J.M., Safi, S., Merrill, S.A., and Ma, P.C. (2021). Immune-Related Adverse Events (irAE) in Cancer Immune Checkpoint Inhibitors (ICI) and Survival Outcomes Correlation: To Rechallenge or Not? Cancers (Basel) *13*, 989.
6. Vonderheide, R.H. (2018). The Immune Revolution: A Case for Priming, Not Checkpoint. Cancer Cell *33*, 563–569.
7. Kahan, S.M., and Zajac, A.J. (2019). Immune Exhaustion: Past Lessons and New Insights from Lymphocytic Choriomeningitis Virus. Viruses *11*, 156.
8. Kyburz, D., Speiser, D.E., Battegay, M., Hengartner, H., and Zinkernagel, R.M. (1993). Lysis of infected cells *in vivo* by antiviral cytolytic T cells demonstrated by release of cell internal viral proteins. Eur. J. Immunol. *23*, 1540–1545.
9. Jamieson, B.D., and Ahmed, R. (1989). T cell memory. Long-term persistence of virus-specific cytotoxic T cells. J. Exp. Med. *169*, 1993–2005.
10. Flatz, L., Hegazy, A.N., Bergthaler, A., Verschoor, A., Claus, C., Fernandez, M., Gattinoni, L., Johnson, S., Kreppel, F., Kochanek, S., et al. (2010). Development of replication-defective lymphocytic choriomeningitis virus vectors for the induction of potent CD8+ T cell immunity. Nat. Med. *16*, 339–345.
11. Cardin, R.D., Bravo, F.J., Pullum, D.A., Orlinger, K., Watson, E.M., Aspoeck, A., Fuhrmann, G., Guirakhoo, F., Monath, T., and Bernstein, D.I. (2016). Replication-defective lymphocytic choriomeningitis virus vectors expressing guinea pig cytomegalovirus gB and pp65 homologs are protective against congenital guinea pig cytomegalovirus infection. Vaccine *34*, 1993–1999.
12. Schwendinger, M., Thiry, G., De Vos, B., Leroux-Roels, G., Bruhwyler, J., Huygens, A., Ganeff, C., Buchinger, H., Orlinger, K.K., Pinschewer, D.D., et al. (2022). A Randomized Dose-Escalating Phase I Trial of a Replication-Deficient Lymphocytic Choriomeningitis Virus Vector-Based Vaccine Against Human Cytomegalovirus. J. Infect. Dis. *225*, 1399–1410.
13. Schmidt, S., Mengistu, M., Daffis, S., Ahmadi-Erber, S., Deutschmann, D., Grigoriev, T., Chu, R., Leung, C., Tomkinson, A., Uddin, M.N., et al. (2023). Alternating arenavirus vector immunization generates robust polyfunctional genotype cross-reactive HBV-specific CD8 T cell responses and high anti-HBs titers. J. Infect. Dis. jiad340.
14. Kallert, S.M., Darbre, S., Bonilla, W.V., Kreutzfeldt, M., Page, N., Müller, P., Kreuzaler, M., Lu, M., Favre, S., Kreppel, F., et al. (2017). Replicating viral vector platform exploits alarmin signals for potent CD8(+) T cell-mediated tumour immunotherapy. Nat. Commun. *8*, 15327.
15. Schmidt, S., Bonilla, W.V., Reiter, A., Stemeseder, F., Kleissner, T., Oeler, D., Berka, U., El-Gazzar, A., Kiefmann, B., Schulha, S.C., et al. (2020). Live-attenuated lymphocytic choriomeningitis virus-based vaccines for active immunotherapy of HPV16-positive cancer. Oncoimmunology *9*, 1809960.
16. A Study of TheraT® Vector(s) Expressing HPV 16+ in Patients With HPV 16+ Confirmed Cancers. https://ClinicalTrials.gov/show/NCT04180215.
17. Jackson, I.J., Chambers, D.M., Tsukamoto, K., Copeland, N.G., Gilbert, D.J., Jenkins, N.A., and Hearing, V. (1992). A second tyrosinase-related protein, TRP-2, maps to and is mutated at the mouse slaty locus. EMBO J. *11*, 527–535.
18. Ring, S., and Flatz, L. (2016). Generation of Lymphocytic Choriomeningitis Virus Based Vaccine Vectors. Methods Mol. Biol. *1404*, 351–364.
19. Hovav, A.H., Panas, M.W., Rahman, S., Sircar, P., Gillard, G., Cayabyab, M.J., and Letvin, N.L. (2007). Duration of antigen expression *in vivo* following DNA immunization modifies the magnitude, contraction, and secondary responses of CD8+ T lymphocytes. J. Immunol. *179*, 6725–6733.
20. Landsberg, J., Kohlmeyer, J., Renn, M., Bald, T., Rogava, M., Cron, M., Fatho, M., Lennerz, V., Wölfel, T., Hölzel, M., and Tüting, T. (2012). Melanomas resist T-cell therapy through inflammation-induced reversible dedifferentiation. Nature *490*, 412–416.
21. Guyonneau, L., Murisier, F., Rossier, A., Moulin, A., and Beermann, F. (2004). Melanocytes and pigmentation are affected in dopachrome tautomerase knockout mice. Mol. Cell. Biol. *24*, 3396–3403.
22. Curtsinger, J.M., Lins, D.C., and Mescher, M.F. (2003). Signal 3 determines tolerance versus full activation of naive CD8 T cells: dissociating proliferation and development of effector function. J. Exp. Med. *197*, 1141–1151.
23. Swiecki, M., and Colonna, M. (2010). Unraveling the functions of plasmacytoid dendritic cells during viral infections, autoimmunity, and tolerance. Immunol. Rev. *234*, 142–162.
24. Gajewski, T.F. (2015). The Next Hurdle in Cancer Immunotherapy: Overcoming the Non-T-Cell-Inflamed Tumor Microenvironment. Semin. Oncol. *42*, 663–671.
25. Srivastava, S., Koch, M.A., Pepper, M., and Campbell, D.J. (2014). Type I interferons directly inhibit regulatory T cells to allow optimal antiviral T cell responses during acute LCMV infection. J. Exp. Med. *211*, 961–974.
26. Li, F., Li, C., Cai, X., Xie, Z., Zhou, L., Cheng, B., Zhong, R., Xiong, S., Li, J., Chen, Z., et al. (2021). The association between CD8+ tumor-infiltrating lymphocytes and the clinical outcome of cancer immunotherapy: A systematic review and meta-analysis. EClinicalMedicine *41*, 101134.
27. Liu, Z., Li, J.P., Chen, M., Wu, M., Shi, Y., Li, W., Teijaro, J.R., and Wu, P. (2020). Detecting Tumor Antigen-Specific T Cells via Interaction-Dependent Fucosyl-Biotinylation. Cell *183*, 1117–1133.e19.
28. Jiang, W., He, Y., He, W., Wu, G., Zhou, X., Sheng, Q., Zhong, W., Lu, Y., Ding, Y., Lu, Q., et al. (2020). Exhausted CD8+T Cells in the Tumor Immune Microenvironment: New Pathways to Therapy. Front. Immunol. *11*, 622509.
29. Kumar, A., Watkins, R., and Vilgelm, A.E. (2021). Cell Therapy With TILs: Training and Taming T Cells to Fight Cancer. Front. Immunol. *12*, 690499.
30. Ping, Y., Liu, C., and Zhang, Y. (2018). T-cell receptor-engineered T cells for cancer treatment: current status and future directions. Protein Cell *9*, 254–266.
31. Black, S., Phillips, D., Hickey, J.W., Kennedy-Darling, J., Venkataraaman, V.G., Samusik, N., Goltsev, Y., Schürch, C.M., and Nolan, G.P. (2021). CODEX multiplexed tissue imaging with DNA-conjugated antibodies. Nat. Protoc. *16*, 3802–3835.
32. zur Hausen, H. (2002). Papillomaviruses and cancer: from basic studies to clinical application. Nat. Rev. Cancer *2*, 342–350.
33. Chang, M.H., Shau, W.Y., Chen, C.J., Wu, T.C., Kong, M.S., Liang, D.C., Hsu, H.M., Chen, H.L., Hsu, H.Y., and Chen, D.S.; Taiwan Childhood Hepatoma Study Group (2000). Hepatitis B vaccination and hepatocellular carcinoma rates in boys and girls. JAMA *284*, 3040–3042.
34. Chen, D.S., and Mellman, I. (2017). Elements of cancer immunity and the cancer-immune set point. Nature *541*, 321–330.
35. Hervas-Stubbs, S., Mancheño, U., Riezu-Boj, J.I., Larraga, A., Ochoa, M.C., Alignani, D., Alfaro, C., Morales-Kastresana, A., Gonzalez, I., Larrea, E., et al. (2012). CD8 T cell priming in the presence of IFN-alpha renders CTLs with improved responsiveness to homeostatic cytokines and recall antigens: important traits for adoptive T cell therapy. J. Immunol. *189*, 3299–3310.
36. Curran, M.A., Montalvo, W., Yagita, H., and Allison, J.P. (2010). PD-1 and CTLA-4 combination blockade expands infiltrating T cells and reduces regulatory T and

myeloid cells within B16 melanoma tumors. Proc. Natl. Acad. Sci. USA *107*, 4275–4280.

37. Kawakami, Y., Dang, N., Wang, X., Tupesis, J., Robbins, P.F., Wang, R.F., Wunderlich, J.R., Yannelli, J.R., and Rosenberg, S.A. (2000). Recognition of shared melanoma antigens in association with major HLA-A alleles by tumor infiltrating T lymphocytes from 123 patients with melanoma. J. Immunother. *23*, 17–27.
38. Berner, F., Niederer, R., Luimstra, J.J., Pop, O.T., Jochum, A.K., Purde, M.T., Hasan Ali, O., Bomze, D., Bauer, J., Freudenmann, L.K., et al. (2021). Keratinocyte differentiation antigen-specific T cells in immune checkpoint inhibitor-treated NSCLC patients are associated with improved survival. Oncoimmunology *10*, 2006893.
39. Nathan, P., Hassel, J.C., Rutkowski, P., Baurain, J.F., Butler, M.O., Schlaak, M., Sullivan, R.J., Ochsenreither, S., Dummer, R., Kirkwood, J.M., et al. (2021). Overall Survival Benefit with Tebentafusp in Metastatic Uveal Melanoma. N. Engl. J. Med. *385*, 1196–1206.
40. Dudley, M.E., Wunderlich, J.R., Robbins, P.F., Yang, J.C., Hwu, P., Schwartzentruber, D.J., Topalian, S.L., Sherry, R., Restifo, N.P., Hubicki, A.M., et al. (2002). Cancer regression and autoimmunity in patients after clonal repopulation with antitumor lymphocytes. Science *298*, 850–854.
41. Geukes Foppen, M.H., Donia, M., Svane, I.M., and Haanen, J.B.A.G. (2015). Tumor-infiltrating lymphocytes for the treatment of metastatic cancer. Mol. Oncol. *9*, 1918–1935.
42. Rohaan, M.W., van den Berg, J.H., Kvistborg, P., and Haanen, J.B.A.G. (2018). Adoptive transfer of tumor-infiltrating lymphocytes in melanoma: a viable treatment option. J. Immunother. Cancer *6*, 102.
43. Yang, J.C. (2015). Toxicities Associated With Adoptive T-Cell Transfer for Cancer. Cancer J. *21*, 506–509.
44. Montague, T.G., Cruz, J.M., Gagnon, J.A., Church, G.M., and Valen, E. (2014). CHOPCHOP: a CRISPR/Cas9 and TALEN web tool for genome editing. Nucleic Acids Res. *42*, W401–W407.
45. Labun, K., Montague, T.G., Gagnon, J.A., Thyme, S.B., and Valen, E. (2016). CHOPCHOP v2: a web tool for the next generation of CRISPR genome engineering. Nucleic Acids Res. *44*, W272–W276.
46. Matter, M., Pavelic, V., Pinschewer, D.D., Mumprecht, S., Eschli, B., Giroglou, T., von Laer, D., and Ochsenbein, A.F. (2007). Decreased tumor surveillance after adoptive T-cell therapy. Cancer Res. *67*, 7467–7476.
47. Tormo, D., Ferrer, A., Bosch, P., Gaffal, E., Basner-Tschakarjan, E., Wenzel, J., and Tüting, T. (2006). Therapeutic efficacy of antigen-specific vaccination and toll-like receptor stimulation against established transplanted and autochthonous melanoma in mice. Cancer Res. *66*, 5427–5435.
48. Zhu, Z., Singh, V., Watkins, S.K., Bronte, V., Shoe, J.L., Feigenbaum, L., and Hurwitz, A.A. (2013). High-avidity T cells are preferentially tolerized in the tumor microenvironment. Cancer Res. *73*, 595–604.
49. Euhus, D.M., Hudd, C., LaRegina, M.C., and Johnson, F.E. (1986). Tumor measurement in the nude mouse. J. Surg. Oncol. *31*, 229–234.
50. Tomayko, M.M., and Reynolds, C.P. (1989). Determination of subcutaneous tumor size in athymic (nude) mice. Cancer Chemother. Pharmacol. *24*, 148–154.
51. Schurch, C.M., Bhate, S.S., Barlow, G.L., Phillips, D.J., Noti, L., Zlobec, I., Chu, P., Black, S., Demeter, J., McIlwain, D.R., et al. (2020). Coordinated Cellular Neighborhoods Orchestrate Antitumoral Immunity at the Colorectal Cancer Invasive Front. Cell *182*, 1341–1359.e19.
52. Kennedy-Darling, J., Bhate, S.S., Hickey, J.W., Black, S., Barlow, G.L., Vazquez, G., Venkataraaman, V.G., Samusik, N., Goltsev, Y., Schürch, C.M., and Nolan, G.P. (2021). Highly multiplexed tissue imaging using repeated oligonucleotide exchange reaction. Eur. J. Immunol. *51*, 1262–1277.
53. Phillips, D., Matusiak, M., Gutierrez, B.R., Bhate, S.S., Barlow, G.L., Jiang, S., Demeter, J., Smythe, K.S., Pierce, R.H., Fling, S.P., et al. (2021). Immune cell topography predicts response to PD-1 blockade in cutaneous T cell lymphoma. Nat. Commun. *12*, 6726.
54. Wang, Y.X., Holbrook, C.A., Hamilton, J.N., Garoussian, J., Afshar, M., Su, S., Schürch, C.M., Lee, M.Y., Goltsev, Y., Kundaje, A., et al. (2022). A single cell spatial temporal atlas of skeletal muscle reveals cellular neighborhoods that orchestrate regeneration and become disrupted in aging. Preprint at bioRxiv. https://doi.org/10.1101/2022.06.10.494732.
55. Sierro, S.R., Donda, A., Perret, R., Guillaume, P., Yagita, H., Levy, F., and Romero, P. (2011). Combination of lentivector immunization and low-dose chemotherapy or PD-1/PD-L1 blocking primes self-reactive T cells and induces anti-tumor immunity. Eur. J. Immunol. *41*, 2217–2228.
56. Schmittgen, T.D., and Livak, K.J. (2008). Analyzing real-time PCR data by the comparative C(T) method. Nat. Protoc. *3*, 1101–1108.